AMERICAN SCIENTIFIC PUBLISHERS

Science of Advanced Materials
Vol. 9, pp. 1–13, 2017
www.aspbs.com/sam

ARTICLE

Optimizing Physio-Mechanical Properties of Halloysite Reinforced Polyurethane Nanocomposites by Taguchi Approach

Tayser Sumer Gaaz[1,2,*], Abu Bakar Sulong[1,*], Abdul Amir H. Kadhum[3], Mohamed H. Nassir[4], and Ahmed A. Al-Amiery[3]

[1]*Department of Mechanical and Materials Engineering, Faculty of Engineering and Built Environment, University Kebangsaan Malaysia, Bangi, Selangor 43600, Malaysia*
[2]*Department of Machinery Equipment Engineering Techniques, Technical College Al-Musaib, Al-Furat Al-Awsat Technical University, Al-Musaib, Babil 51009, Iraq*
[3]*Department of Chemical and Process Engineering, Faculty of Engineering and Built Environment, Universiti Kebangsaan Malaysia, Bangi, Selangor 43600, Malaysia*
[4]*Program of Chemical Engineering, Taylor's University-Lakeside Campus, Subang Jaya, Selangor 47500, Malaysia*

ABSTRACT

The vast and multi-oriented applications of pure TPU firmly stand in industrial and research fields. To further and deeper applications in these fields, TPU has been loaded as a host polymer with HNTs, in particular, to develop very well and attractive engineering materials that are commonly known as nanocomposites. In order to achieve the best results with minimum cost, Taguchi's approach was heavily used in labs as well as in industry. In this work, it is not only Taguchi analysis was used, but also ANOVA statistical approach to, further, fortify the analysis. Under the concept of using the two approaches, side-by-side, the results could be considered more reliable findings. Based on Taguchi approach, three levels for preparing TPU-HNTs nanocomposites were employed as follows: mixing temperature (190, 200, 210 °C); mixing speed (30, 40, 50 rpm); mixing time (20, 30, 40 min); and loading (1, 2, 3 wt.% HNTs). The controlled parameters and their three relevant levels were employed to test the response characterized by tensile strength, Young's modulus, and tensile strain. The most important results in this work were found to be loading TPU with only 1 wt.% HNTs which has improved the tensile strength and tensile strain by 44% and 144%, respectively. This improvement using the delicate parameters as chosen levels has outperformed all known results up-to-date. Surprisingly, however, the TPU crystal has shown very limited deformation as the field emission scanning electron microscope (FESEM) and thermogravimetric analyses (TGA) have suggested. The images at the fracture surface of TPU-HNT's samples taken by the FESEM have shown that the agglomeration could be the reason behind the insignificant effect of more HNTs loading.

KEYWORDS: Nanocomposite, Design-of-Experiment, Taguchi Optimization Method, Mechanical Properties.

1. INTRODUCTION

Unique inorganic filler, halloysite nanotubes (HNTs), chemical structure of $Al_2Si_2O_5(OH)_4 \cdot nH_2O$, apparently belongs to the kaolin family. HNTs is considered to be one of the components of polymer nanocomposite material in addition to nanoclay material and aluminium filler. Currently, there is no standard method of producing HNTs, which results in having HNTs in a variety of geometric sizes ranging between 300 and 1500 nm in length, 15 to 100 nm in inner diameter and 40 to 120 nm in outer diameter.[1,2] Generally, HNTs possesses important characteristics such as enhancing thermal stability, impeding crack growth, and strengthening the mechanical properties of the matrix of nanocomposites.[3] In addition, the relatively cheap HNTs shares its counterpart, carbon nanotubes CNTs, similar characteristics of a longitudinal hollow structure which allows it to form layers of tetrahedral sheets of silica and octahedral sheets of alumina.[1,4,5] For these reasons, the applications of HNTs extend to include cosmetics reinforcement, catalyst carriers, and drug delivery due to its unusual shape and geometry, surface properties, chemical formation and cost-efficiency.[6] In this paper, HNTs is reinforced as filler with thermoplastic

*Authors to whom correspondence should be addressed.
Emails: taysersumer@gmail.com, abubakar@ukm.edu.my
Received: xx Xxxx xxxx
Accepted: xx Xxxx xxxx

polyurethane (TPU). TPU, which is available with a wide range of hardness,[7] is a thermoplastic material with excellent physio mechanical properties such as high tensile strength and strain with the characteristic of excellent abrasion resistance.

The host polymer, TPU, has unique physical–chemical properties in addition to versatility, which strengthens the importance of this material in many applications.[8] TPU has recently been investigated and, along with its preparation techniques, the physical and chemical properties were tested and improved.[9] The development of new composites through employing an internal mixer requires proper settings for such parameters as mixing temperature, speed, time, and the loading of the thermoplastic with the HNTs filler in order to optimize these parameters to achieve the best results.[10, 11] Gholami and Sadeghi[12] studied different nanoclays of TPU-clay nanocomposites via melting the mixture, and their findings showed that these materials have a very close dispersion to exfoliation.[12] In another study, Shokoohi et al.[13] found that the mixing parameters affect the average particle size as, for example, the twin screw extruder produces smaller particles with a more narrow distribution of sizes than the single screw extruder.[13]

The formation of TPU-HNTs nanocomposites involves implementing several parameters in the mixing process, which makes optimizing very difficult to achieve. The delicacy of the process is tied to the designing of a number of trials for optimization. Currently, there have been a few attempts to reduce the required number of trials without affecting the qualities of the experimentation. One of these attempts was statistically formalized by Taguchi in the late 1940s.[14] Taguchi proposed such a design for a system of experiments to achieve optimization with a reasonable number of trials. In this regard, the Taguchi designing method starts with selecting specific control factors. To achieve this optimization, Taguchi proposed an experimental plan in terms of orthogonal arrays (OAs), which include different combinations of parameters in conjunction with their levels for each trial, suggesting that the entire parameter space could be performed with a minimum number of trials.[13, 15] Interaction among factors could be determined and a lesser number of experiments would be needed to get the desired accuracy.[16]

There are two approaches for maximizing the controlled parameters: static and dynamics. In static approach, the noise and the controlled parameters are fed together for processing the output. In the dynamic approach, the noise, the controlled parameters, and an external noise are fed together for processing the output. In this current work, the static approach was employed for simplicity. Mixing parameters yield a response which appears as noise. Statistically, the noise measurement is conducted according to several schemes. In this work, the scheme chosen is "larger is better" where the response is maximized and the output is positive always according to $S/N = -10 \log \sum(1/y^2)/n$.

Accordingly, the number of trials in the current plan, based on Taguchi L_9 orthogonal arrays, has been reduced to only nine[13] out of the 27 trials in the traditionally employed techniques. Traditionally, for instance, a set of three experiments with three trials for each requires 27 trials, which, apparently, is difficult, costly, and time-consuming to conduct within the industry. The Taguchi method of design-of-experiment (DOE) has been used for quite some time to improve products, manufacturing processes and, more specifically, challenging quality problems. The Taguchi method of analysis in conjunction with statistical experimental design has become popular based on the most recent work[17–19] and is a widely used technique for optimization and improving qualities.[20] The outcome of using the Taguchi method is the optimization of the manufacturing process and design.[21–23]

The current study has shown that there are promising research techniques to improve TPU by mixing it with HNTs. However, nanocomposites still face major drawbacks in procedures, which could be caused by adopting trial-and-error for achieving reliable results for improvement. In order to soften this drawback, the Taguchi method has been heavily used not only to reduce the number of experiments but also to strictly curb the trial-and-error principle by proposing the best parameters to achieve the purpose.

The execution of the experiment must take the inherent variability of the materials into account. The aim of this work is to explore how mixing parameters influence the mechanical properties of TPU-HNTs nanocomposites using the best conditions predicted by utilizing the Taguchi statistical method to obtain the optimum conditions for the best mechanical properties.

2. RESULTS AND DISCUSSION

2.1. Characterization of Neat HNTs

2.1.1. TEM

The neat HNTs without the addition of TPU was investigated using low and high magnification TEM at 100 kV, as shown in Figures 1(a) and (b), respectively. The basic purpose of the TEM tests was to identify the HNTs structure. At a lower magnification, a group of nanotubes appeared at different lengths and diameters, as shown in Figure 1(a). In order to have a better understanding of accurate dimensions, TEM images were taken at a high magnification. These images enabled us to measure, with the best accuracy, the dimensions of each nanotube. A typical measurement showed that the inner diameter of the nanotubes was 16.02 nm while the outer diameter was 55.89 nm. These measurements are within the range that was suggested by other studies of 10–30 nm and 50–100 nm, for inner and outer diameters, respectively. The TEM images also showed that the nanotubes were agglomerated in various groups with various sizes and arbitrary orientations.

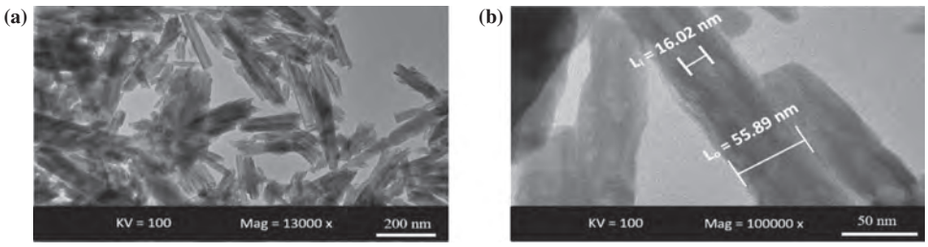

Fig. 1. TEM images of neat HNTs: (a) at 13k× (low magnification), and (b) 100k× (high magnification).

2.1.2. FESEM

The topography of the surface of the neat HNTs was investigated by FESEM at low and high magnification, as shown in Figures 2(a) and (b), respectively. FESEM images depict an in-depth-investigation of the HNTs block matrix. The FESEM images of homogeneously dispersed neat HNTs at a lower magnification is shown in Figure 2(a) and at a higher magnification in Figure 2(b).

2.1.3. TGA

The TGA curve of the thermal treatment of the neat HNTs shows two distinctive stages of weight loss; the first occurs immediately at about 30 °C suggesting that the unbound water is evaporated. This stage extends to about 400 °C at which the rate of weight loss increased significantly from 0.0111/°C to 0.097/°C-about 9 times that of the first stage. The different rate of weight loss suggests that water binds to the HNTs structure at different levels. Regarding the first stage, HNTs allows a very weakly held monolayer of water molecules, which is located about 7 Å from the surface, to evaporate.[24] The other stage, which requires higher temperatures to liberate water, could refer to the water molecules which are sitting between two consecutive layers, which makes desorbing water much more difficult than in the previous stage.[25] The high second stage weight loss rate might be attributed to some structural changes due to a high temperature–a case that needs more study and is beyond the scope of this paper. At a transitional temperature between the first and the second stage (about 400 °C), HNTs undergoes a faster degradation, which is shown clearly in Figure 3.

2.2. Taguchi Analysis of TPU-HNTs Nanocomposites

The experimental procedure and the relevant results are well-guided by the Taguchi's DOE. DOE is a very powerful approach that offers very delicate and accurate guidance for minimizing the number of experiments and optimizing the performance of the experiment. In the following sections, a detailed procedure for the calculation of the mechanical properties of TPU-HNTs nanocomposite is presented.

2.2.1. Selecting the Processing Parameters

The selection of experimental parameters, known as controlled factors, is conducted carefully based on previous work in the same field and due to extending the experimental scope. Some parameters are tightly connected to the physical and chemical properties of the material under investigation such as the melting temperature and density. For the temperature, TPU-HNTs nanocomposites were prepared at selected temperatures of 190, 200, and 210 °C which differ slightly from the published works of El-Shekeil et al.[10] due to different characteristics of the TPU-HNTs preparation. Temperatures above 210 °C are critical for neat TPU due to the unavoidable thermal degradation of the neat TPU, as suggested by the manufacturer. The temperature of 210 °C is slightly lower than the critical temperature proposed by El-Shekeil et al.[10] whose team experimented samples of different origin and, as such, different impurities could be found. The second controlled parameter is the speed of the mixing process. Three speeds are selected at 30, 40, and 50 rpm based on the manufacturer recommendation and available information from previous work[10] who concluded that low speeds do not produce a homogenous mixture while high speeds may

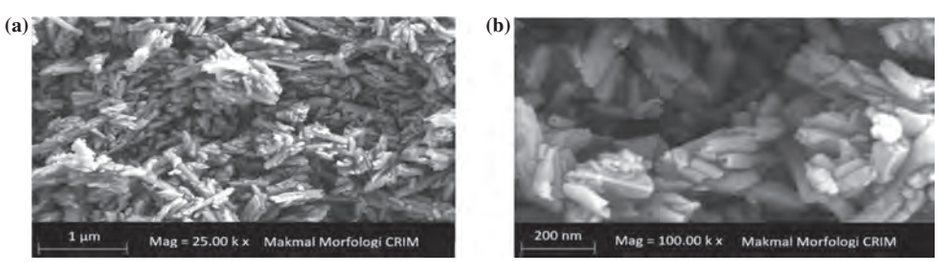

Fig. 2. FESEM microphotographs for neat HNTs (a) low magnification and (b) high magnification.

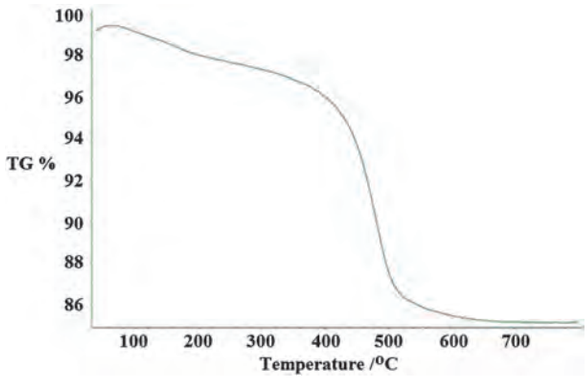

Fig. 3. TGA curve of neat HNTs.

cause breakage of filler.[10] The third controlled parameter is the time intervals of the mixing process. Three-time levels were chosen at 20, 30, and 40 min based on observing the torque in the mixer since torque is a good indicator for how well the mixture is prepared.[10] It was suggested that if the torque has not stabilized, the ingredients are not sufficiently mixed-a case that leads to poor dispersion. On the other hand, the more time following the torque stabilization of the mixture, the more thermal degradation and breakage of the mixture will have occurred.[10] In addition, TPU-HNTs nanocomposites could also break due to shear stress and temperature which, among other reasons, affects the overall performance of the composite, as suggested by El-Shekeil et al.[10] The last parameter taken into account was HNTs loading (based on wt.%). As in the preparation of alloys or semiconductors, the additive loadings are very small ratios which go very well in case of TPU-HNTs preparation. Based on previous work,[26] loading was performed within wt. ratios of no more 10 wt.%.[26] The selection of 1, 2, and 3 wt.% HNT is very reasonable for early characterization of TPU-HNTs nanocomposites. Table I contains the controlled factors and their relevant levels.

The total number of trials as suggested by the Taguchi method design is 9 as shown in Table II, where all controlled parameters are shown. In the following paragraphs, the experiments suggested above are conducted and the relevant results are shown therein.

2.2.2. Tensile Properties

TPU-HNTs nanocomposite samples were tested for tensile properties. Nine runs were prepared according to the criteria in Tables I and II and the tensile strength, Young's modulus, and the tensile strain was calculated and shown in Table III. Each of the nine runs was divided into three similar pieces and the S/N's were calculated according to the criteria of "larger is better" which is explained in Appendix A. to find the average of each experimented response of tensile strength, Young's modulus, and tensile strain. The results of the average of each response and its relevant S/N values for mixing temperatures at level I (items 1, 2, and 3); level II (items 4, 5, and 6); and finally at level III (items 7, 8, and 9) are listed in Table IV. Similar tables can be generated for the other factors of mixing speed, mixing time, and HNTs loading as described earlier.

In previous calculations of S/N, each response was evaluated based on the maximization of parameters depicted by Taguchi's design as shown in in Table II. The average S/N values are calculated based on Taguchi's predictions of the maximizing parameters and were not involved the effect of the each level. Table IV shows only the maximum values depicted and organized based Levels I, II, or III for each response. Despite this classification, the results in Table IV are not conclusive because it is not easy to characterize the effect of the Level on each response.

The highest and the lowest results in Table IV are re-tabulated in Table V to show the effects of the

Table I. The parameters for three levels of selected factors.[7, 10, 12, 26–30]

Controlled factors	Level 1	Level 2	Level 3
Mixing temperature (°C)	190	200	210
Mixing speed (rpm)	30	40	50
Mixing time (min)	20	30	40
HNTs loading (wt.%)	1	2	3

Table II. Effective combination parameters suggested by Taguchi (L_9).

Trial no.	Mixing temp. (°C)	Mixing speed (rpm)	Mixing time (min)	HNTs loading (wt.%)
1	190	30	20	1
2	190	40	30	2
3	190	50	40	3
4	200	30	30	3
5	200	40	40	1
6	200	50	20	2
7	210	30	40	2
8	210	40	20	3
9	210	50	30	1

Table III. Tensile experimental results for mixing temperatures.

	Tensile strength (MPa)		Young's modulus (MPa)		Tensile strain (%)	
Experiment no.	Average	S/N	Average	S/N	Average	S/N
Neat TPU	17.70	–	2.30	–	430.30	–
1	25.25	28.04	3.45	10.77	1050.72	60.42
2	19.17	25.65	6.54	16.31	990.46	59.91
3	15.79	23.97	10.53	20.45	608.20	55.68
4	16.79	24.50	10.12	20.10	680.76	56.66
5	19.05	25.60	7.77	17.81	1015.50	60.13
6	17.54	24.88	8.05	18.12	870.13	58.79
7	21.24	26.54	6.05	15.64	1005.93	60.05
8	13.13	22.36	11.54	21.24	508.63	54.12
9	21.13	26.50	5.63	15.01	1030.50	60.26

Table IV. Average S/N ratio values for tensile properties.

Parameter	Mixing temp. (°C)	Mixing speed (rpm)	Mixing time (min)	HNTs loading (wt.%)
Tensile strength (MPa)				
Level I	25.89	26.37	25.10	26.72
Level II	25.00	24.54	25.55	25.70
Level III	25.14	25.12	25.37	23.61
Young's modulus (MPa)				
Level I	15.85	15.51	16.71	14.54
Level II	18.68	18.46	17.15	16.69
Level III	17.30	17.87	17.97	20.60
Tensile strain (%)				
Level I	58.68	59.05	57.78	60.27
Level II	58.53	58.06	58.95	59.59
Level III	58.15	58.24	58.62	55.49

controlled parameters correlated with their corresponding levels. Apparently, the highest values are mostly occurring at the level I (Table I) by showing 9 cases out of 16 possible cases for this level. For the lowest values of the responses, there are only 6 occurrences out of 16 total cases. Physically, the highest tensile strength is the lowest Young's modulus, and vice versa since the perfectly rigid material has infinite Young's modulus while the rubber, which has very low young's modulus, is very high in tensile strength.[31] This important result shows that the same controlled parameters affect oppositely these two parameters. Table V shows that the least possible effective level for highest or lowest response appears at level II.

It is very important to note that the responses measurements based on "Larger is Better" criteria to evaluate S/N ratios for each controlled parameters are graphically shown for tensile strength, Young's modulus, and tensile strain in Figures 4–6, respectively. The graphical representation of the results shows the highest, the lowest and the middle effect of each level of the controlled parameters on the response. The choice of these effects is concluded by the software rather than direct observations.

In a parallel analysis, the average S/N ratios of the responses were investigated in accordance with the levels I, II, and III as shown in Table V. The results show that the tensile strength is highly influenced by level I mixing temperature of 190 °C, level I of mixing speed of 30 rpm, level II of mixing time of 30 min, and level I of HNTs loading of 1 wt.%. Young's modulus is highly influenced by level III of mixing temperature of 210 °C, level II of mixing speed of 40 rpm, level II of mixing time of 30 min, and level III of HNTs loading of 3 wt.%. The tensile strength is highly influenced by level I of mixing temperature of 190 °C, level I of mixing speed of 30 rpm, level II of mixing time of 30 min, and level I of HNTs loading of 1 wt.%.

Table V. The highest and lowest values of the responses and their relevant parameters.

	Tensile strength				Young's modulus				Tensile strain			
Parameter	High		Low		High		Low		High		Low	
Mixing temperature (°C)	I	190	III	210	III	210	I	190	I	190	III	210
Mixing speed (rpm)	I	30	II	40	II	40	I	30	I	30	II	40
Mixing time (min)	I	20	I	20	I	20	I	20	I	20	I	20
HNTs loading (wt.%)	I	1	III	3	III	3	I	1	I	1	III	3

The results analysed by Taguchi method show how each of the three responses under investigation is influenced by a certain controlled parameter or the any given individual level. The analysis is not comprehensive due to the fact that the highest (the lowest) values could take place with some controversy. In order to remove these controversial results, ANOVA was employed for further characterization. In ANOVA, the average of all responses is evaluated versus each controlled parameter of the three were not good enough to have a very solid conclusion. ANOVA provides the very powerful approach which suggests whether each controlled parameter is significant or not. The data in Table VI were analysed using ANOVA in order to determine the F-ratio and the percentage contribution of each parameter. The results of the sum of squares, the degree of freedom, the mean sum of the squares, F-ratio, and the percentage contribution are listed in Table VI.

The 2-way ANOVA, set at 5% significant, provides analysis for each controlled factor using two important factors, namely, F-ratio and the contribution percentile of each controlled parameter. For tensile strength, the highest contribution comes from loading, followed by mixing speed and then mixing temperature. The contribution of mixing time has a negative effect. The tensile strength is affected mainly by loading, whereby the F-ratio is the highest. The preceding result suggests that HNTs enforces TPU by a factor of about 60%. This result is in good agreement with the other results despite the fact that the improvement is about 40% for loading up to 2 wt.% as experimented by Russo et al.[28] and 64% for nanoclay loaded with 3 wt.% as performed by Pizzatto et al.[26] The significance, measured by the F-ratio, of each factor of mixing temperature, mixing speed, mixing time and loading have a value of 2 wt.% or above which is in agreement with the other results.[10] The results of the ANOVA analysis in Table VI show that the mixing temperature has a contribution of about 6%, which is very small compared to the loading effect. This is in conflict with the findings proposed by El-Shekeil et al.[30] The work was done by El-Shekeil et al.[30] is different as the filler was kenaf-bast-fibre, which is very different from the HNTs used in this work. Kenaf-bast-fibre is considered to be a temperature resistive material and the loading does not show a potential tendency to be an important factor.

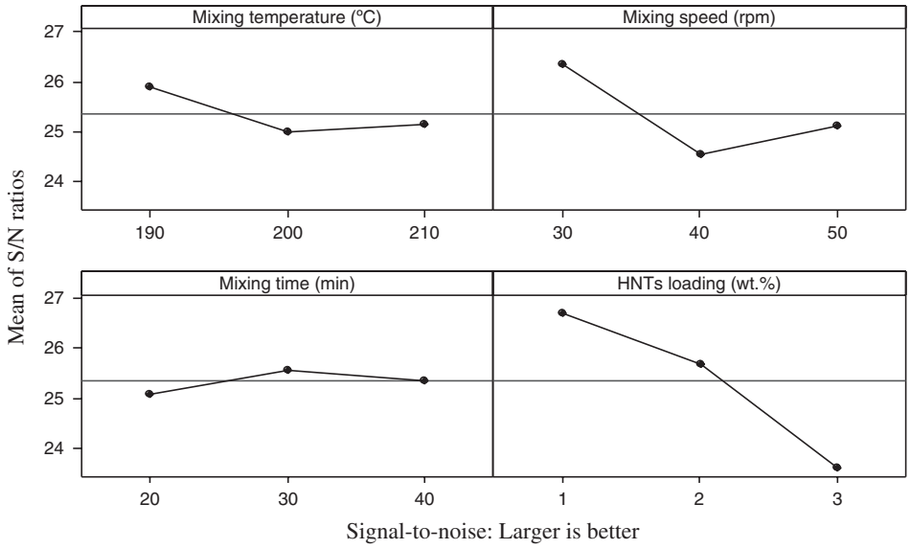

Fig. 4. Main effects plot for S/N ratios on the tensile strength parameter.

2.2.3. Fractured Surfaces of Optimum Tensile Specimen

Four samples were investigated by FESEM: neat TPU, 1 wt.% HNTs loading, 3 wt.% HNTs loading, and a sample at the optimizing parameters of 190 °C, 30 rpm, 30 min, and 1 wt.% HNTs loading. The surface at the fracture of each sample was examined at two magnifications, 1 and 5k×. FESEM is a very useful technique for explaining two features that are related to loading TPU by HNTs. The first feature is about the distribution of HNTs with the host TPU, while the second factor is how well HNTs is distributed within the TPU. Neat TPU was examined first as a reference to demonstrate the fractured surface of neat TPU, as shown in Figures 7(a) and (b) at magnifications of 1 and 5k×, respectively. The surface of TPU did not show any irregularities and the presence of hole-like spots is very normal for plasticity behavior.[32] The TPU 1 wt.% HNTs fractured surface is shown in Figures 7(c) and (d) at magnifications of 1 and 5k×, respectively. The fractured surface at the lower magnification clearly shows the presence of HNTs and its distribution. The image at a higher magnification shows agglomeration of HNTs at certain positions; however, the distribution still looks normal.[26] As the HNTs percentage increases to 3 wt.%, Figure 7(e) shows the presence of more filler in the fractured surface. The image at a higher magnification of 5k× shows bigger area of agglomeration of HNTs. The FESEM images of the last sample, which was prepared at the optimizing parameters, are shown in Figures 7(e) and (f) at a magnification of

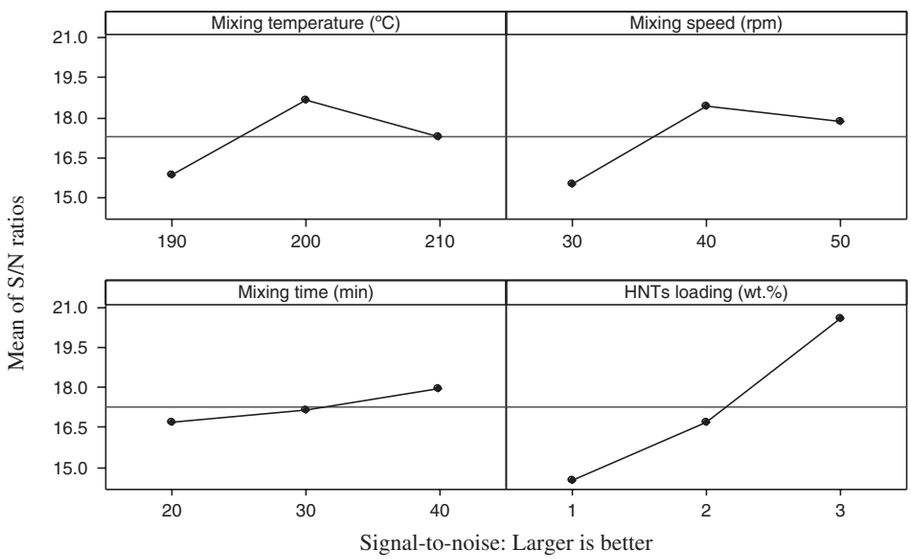

Fig. 5. Main effects plot for S/N ratios on the Young's modulus parameter.

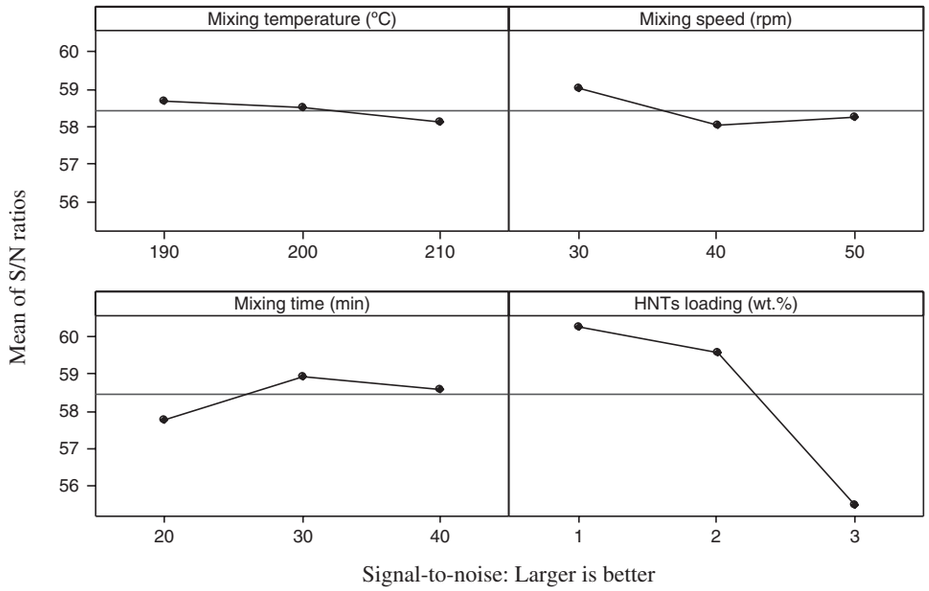

Fig. 6. Main effects plot for S/N ratios on the tensile strain parameter.

1 and 5k×, respectively. The surface looks smoother, the filler is very well distributed, and agglomeration appears at very limited spots.

The fracture surface is another mechanism for the comprehension of the changes in the mechanical properties since the FESEM test is carried out at the fractured part. The shape of the surface suggests, to a high level of certainty, a certain relationship with the strength of the sample. For the TPU sample shown in Figures 7(a) and (b), the tensile strength of 17.7 MPa (Table IV) is very close to the 20 MPa suggested by the manufacturer. The irregularities shown in the fractured surface could play an important role in the tensile strength as suggested by Ref. [33]. The results of 1 wt.% HNTs loading, shown in Table VI, for runs 5 and 9 are 19.05 MPa and 21.13 MPa, respectively. The tensile strength is improved by this loading by 7.6% and 19.5%, respectively. The difference between the results is mainly due to the cross effects of other parameters that contribute to tensile strength, as shown in the ANOVA analysis. When the 3 wt.% HNTs was tested at the fractured surface, the FESEM images in Figures 7(e) and (f) showed, as previously stated, that the sample had more filler; however, the tensile strength decreased to less than that of neat TPU. One possible reason for such a result is that the TPU-HNTs nanocomposites at 3 wt.% become brittle, which means that the tensile strength could be severely reduced.[26] Overall, the results presented in this section and the preceding sections prove that the Taguchi method is an excellent approach to reducing the number of experiments and to proposing the best optimization for the setting.

Table VI. ANOVA average on tensile properties.

Parameter	Mixing temp. (°C)	Mixing speed (rpm)	Mixing time (min)	HNTs loading (wt.%)	Error%
Tensile strength (MPa)					
SS	24.3	76.60	0.81	198.26	29.51
DF	2	2	2	2	–
MS = SS/DF	12.1	38.30	0.40	99.13	1.63
F ratio	7.4	23.36	0.24	60.45	1
%contribution	6.3	22.25	−0.74	59.16	12.93
Young's modulus (MPa)					
SS	14.6	20.89	2.18	127.68	22.01
DF	2	2	2	2	–
MS = SS/DF	7.3	10.44	1.09	63.84	1.22
F ratio	6.0	8.53	0.89	52.19	1
%contribution	6.5	9.83	−0.13	66.80	16.96
Tensile strain (%)					
SS	6075.6	33979.96	39789.68	961112.51	11333.88
DF	2	2	2	2	–
MS = SS/DF	3037.8	16989.98	19894.84	480556.25	629.66
F Ratio	4.8	26.98	31.59	763.19	1
%contribution	0.4	3.10	3.66	91.21	1.55

Notes: SS = sum of square, DF = degree of freedom, MS = mean sum of square, *F* ratio = *F* ratio for each factor, %contribution = percentage contribution.

2.2.4. *Thermogravimetric Analysis of the Optimum Tensile Specimen*

The TGA of the TPU and TPU-HNTs nanocomposites are shown in Figures 8(a)–(d) and the results are tabulated in Table VII. The decomposition of TPU shown in Figure 8(a) occurs at about 290 °C with a 2.34% weight loss due to the decomposition of the urethane matrix, while the second stage is characterized by a 41.11%-weight loss

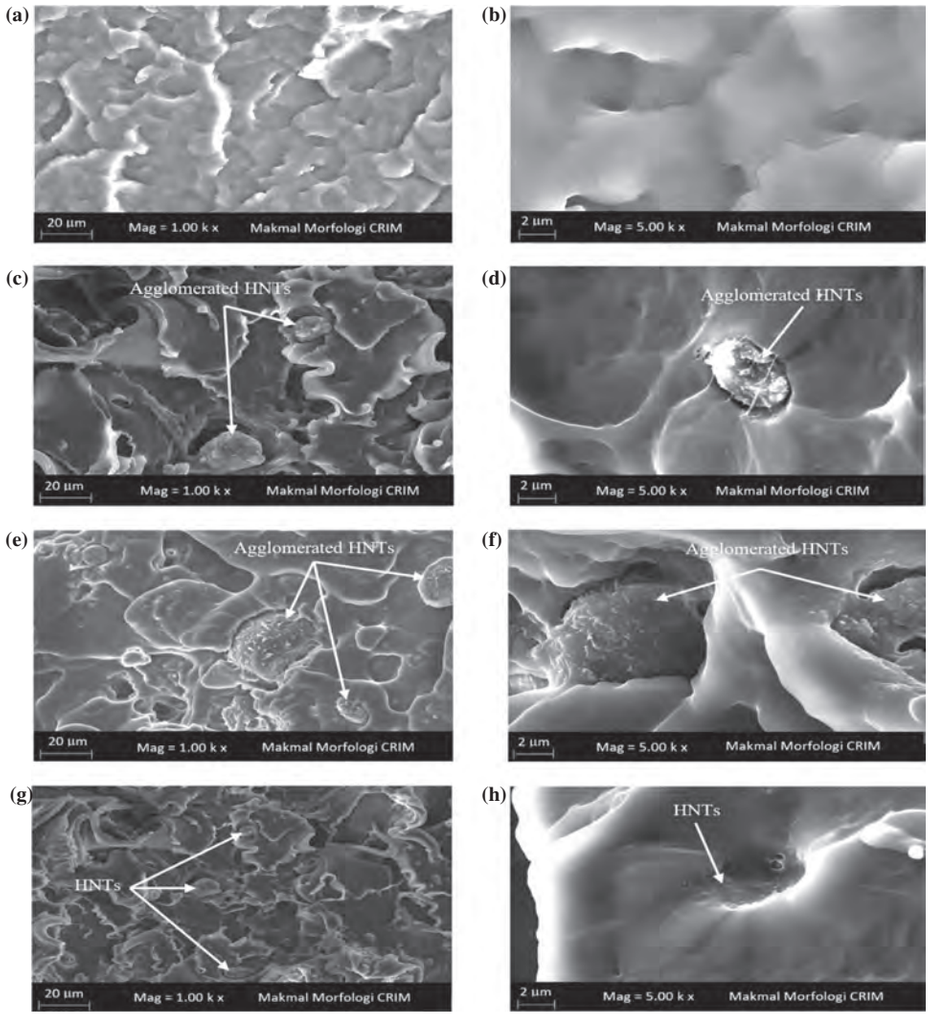

Fig. 7. FESEM showing the uniform dispersion of HNTs in a TPU matrix (a, b) neat TPU, (c, d) 1 wt.%, (e, f) 3 wt.% and (g, h) optimum parameters, with lower magnification of 1.00k× and higher magnification of 5.00k×.

between 290 and 470 °C. These results are slightly different from Ref. [34] due to different composition and optimizing parameters. It can be seen from the curve that the thermal stability of TPU rises as the HNTs loading is increased from 1 to 3 wt.%. Neat TPU starts to degrade at 290 °C and is completely decomposed at around 680 °C, while TPU with 1 to 3 wt.% HNTs starts to degrade at about 280 to about 580 °C, respectively. The weight loss of neat TPU and nanocomposite during the course of the TGA testing was about 84%, compared to about 97% for nanocomposites. Seemingly, the loading with HNTs makes the weight loss faster than in the neat sample. In this regard, HNTs loading has a major role in changing the structural and physical properties of the TPU-HNTs nanocomposites, which might be attributed to possible chemical bonding. The distribution of HNTs throughout the host, TPU, has another effect on the thermal properties of the composite. It is also suggested that the molecular mobility imparted by the HNTs also plays a vital role in this thermal decomposition phenomenon.[35] The degradation, furthermore, is likely the result of the absorption and adsorption of free radicals generated during the TPU degradation process on the active halloysite particle surface of the nanotubes.[12]

2.2.5. Differential Scanning Calorimetry of the Optimum Tensile Specimen

The differential scanning calorimetry (DSC) is a technique that measures the amount of heat required to increase the temperature of a sample and a reference as a function of time or temperature while the reference and the sample are kept nearly at same temperature. As the temperature increases or decreases, the phase transition of the sample could take place at which more (exothermic) or less (endothermic) heat will flow to the sample in order to maintain same temperature. The endothermic phase transition from solid to liquid represents absorption heat by the

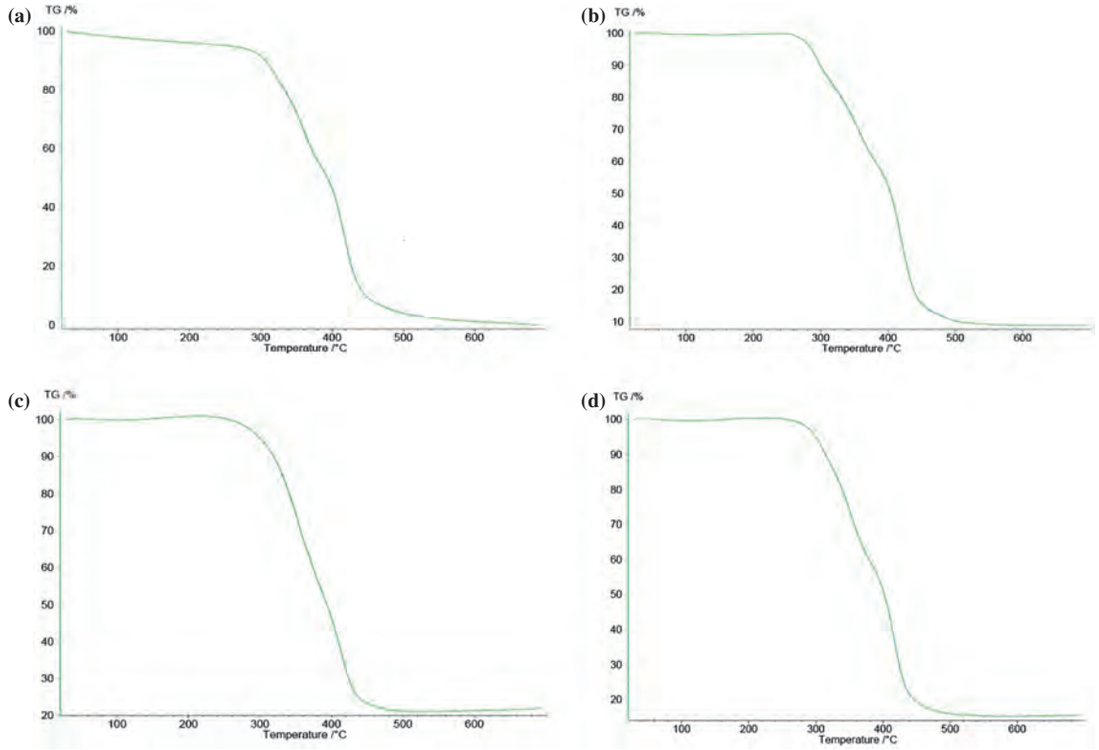

Fig. 8. TGA thermograms of (a) neat TPU, (b) 1 wt.%, (c) 3 wt.%, and (d) optimum parameter wt.% HNTs loading nanocomposites in a nitrogen atmosphere.

sample while exothermic process (crystallization) requires less heat to maintain the sample temperature during this process. The phase transition appears at about 350 °C when the heat is supplied showing a sudden jump in the heat supplied to the sample which occurs at same temperature. Crystallization is associated with full or partial alignment of the molecular chain which reflects the effect on the mechanical stretching of the polymer depending on the degree of crystallinity. In addition to the melting temperature and the crystallization temperature, a glass transition is another temperature can be determined by DSC. The glass transition is very important in industrial settings for quality control instrumentation purposes which is used to show the purity of the polymer. DSC results are shown in Figure 9. There are two DSC runs in each trial: heating (0 °C–300 °C) and cooling (300 °C–0 °C) where glass transition and melting point are determined in the heating part while crystallization temperature is determined in the cooling stage of the experiment.

Table VII. TGA results.

	Degradation stage (1)		Degradation stage (2)		Degradation stage (3)	
Sample	T (°C)	Weight loss%	T (°C)	Weight loss%	T (°C)	Weight loss%
Neat TPU	30–290	2.34	290-470	41.11	470–680	8.57
TPU-1 wt.% HNTs	30–280	0	280–440	51.21	440–580	12.14
TPU-3 wt.% HNTs	30–265	0	265–430	45.45	430–490	20.00
Optimized sample	30–295	0	295–440	52.51	440–490	30.00

The results shown in Figure 9 are summarized in Table VIII. Three stages are recognized: T_g, T_m, and T_c. The T_g is always below the T_m because the T_m requires more heat to occur. The T_g occurs at the peak temperature of 102.77 °C for TPU matrix. As HNTs is loaded to TPU, the T_g significantly decreased to 69.3 °C and seemingly no significant change when HNTs loading increased to 3 wt.% or for the optimum sample. The decrease of T_g from 102.77 to 69.3 °C exhibits a change from rubber-like state of TPU matrix to brittle glassy state of TPU-HNTs nanocomposites. The T_m of TPU matrix was recorded by DSC at 337.51 °C which shows no change for 1 wt.% TPU-HNTs nanocomposites and as HNTs loading increased to 3 wt.%, the T_m increased to 343.46 °C and remains within a small shift for the optimized sample. The third temperature is the T_c which appears at −15.64 °C for TPU matrix and shifted to lower temperature of −22.80 °C for 1 wt.% TPU-HNTs nanocomposites. The crystallization temperature for 3 wt.% TPU-HNTs nanocomposites are shifted to higher temperature of −8.60 °C and −1.68 °C for the optimized sample. The degradation of

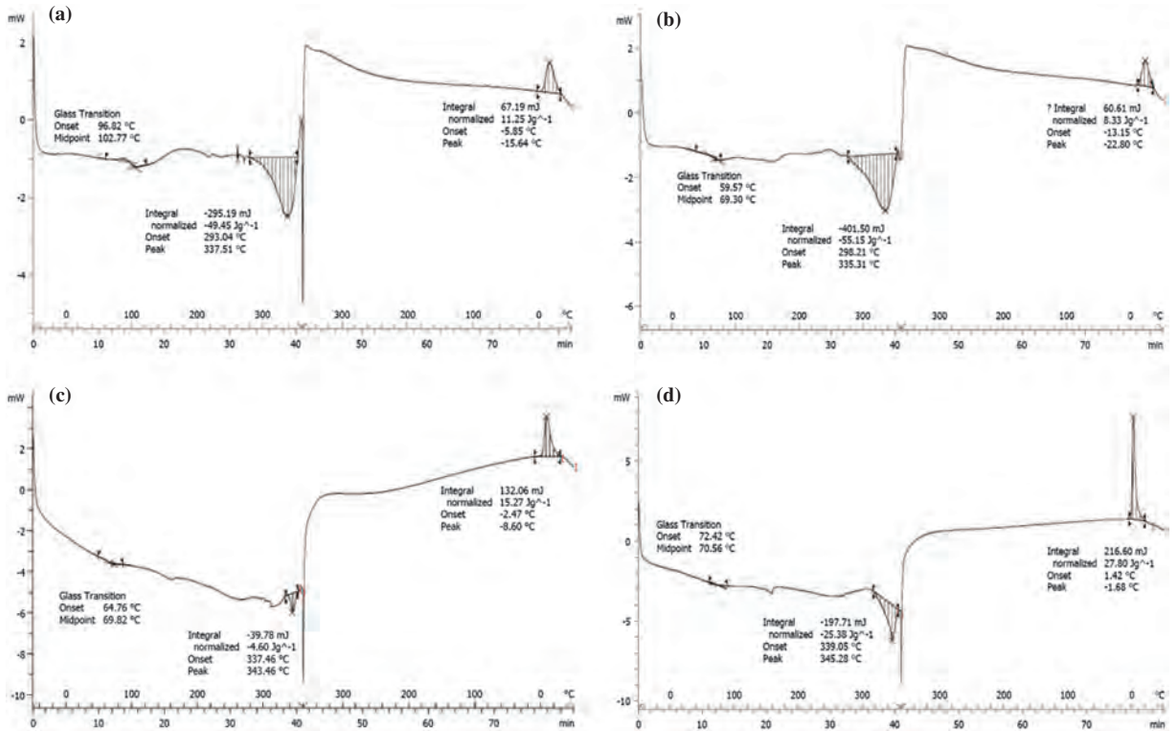

Fig. 9. DSC results (a) neat TPU, (b) 1 wt.%, (c) 3 wt.%, and (d) optimum parameter wt.% HNTs loading nanocomposites.

Table VIII. Summarized DSC result of TPU-HNTs nanocomposites.

	Glass transition temp.			Melting temp.			Crystallization temp.		
Sample	Onset (°C)	Peak (°C)	Integral (mJ)	Onset (°C)	Peak (°C)	Integral (mJ)	Onset (°C)	Peak (°C)	Integral (mJ)
Neat TPU	96.82	102.77	–	293.45	337.51	−295.19	−5.85	−15.64	67.95
TPU-1 wt.% HNTs	59.57	69.30	–	298.21	335.31	−55.15	−13.15	−22.80	60.61
TPU-3 wt.% HNTs	64.76	69.82	–	337.46	343.46	−39.78	−2.47	−8.60	132.06
Optimized Sample	72.42	70.56	–	339.05	345.28	−197.71	1.42	−1.68	216.60

TPU matrix and TPU-HNTs nanocomposites are seen in both investigations of TGA and DSC.

3. MATERIALS AND METHODS

3.1. Materials

TPU (Ester type), in the form of semi round shape bead forms of about 5 mm in diameter, was purchased from Global Innovations-polycarbonates Bayer Material Science AG, D-51368 Leverkusen, as shown in Figure 10(a). The physical properties of TPU are summarized in Table I. HNTs, in powder form with an average size of 20 nm, was purchased from Natural Nano, Inc., 832 Emerson Street, Rochester, New York, as shown in Figure 10(b). The chemical composition of HNTs and the physical properties of HNTs are summarized in Tables IX and X, respectively.

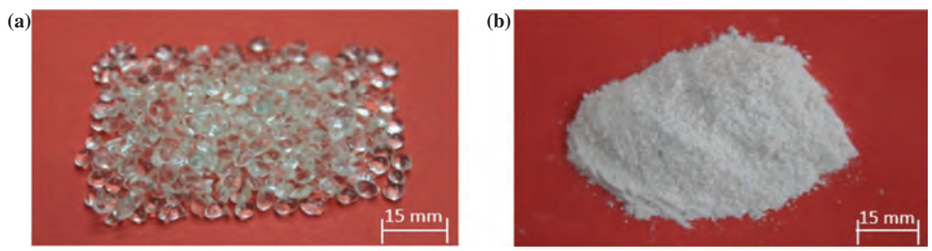

Fig. 10. Manufacturer specifications for (a) TPU, and (b) HNTs.

Table IX. Chemical composition of HNTs.

Chemical compositions	SiO_2	Al_2O_3	TiO_2	Impurities
Weight %	61.19	18.11	20.11	< 0.5%

3.2. Instrumentation

Transmission Electron Microscopy (TEM), using a Philips CM12 Somerset, New Jersey, US), operated at 80 kV and producing an electron beam capable of interacting with the sample as it passes through, was used to provide images showing the existence of the nanotubes. TEM is used in many fields in science, engineering and medicine to examine the nanotube details at the surface. In this report, TEM was used to identify and locate the nanotubes and to measure the geometrical dimensions of their inner and outer diameters. In addition to TEM, a FESEM, model ZEISS SUPRA 55-VP (Manufacturer, Konigsallee, Deutschland) with a magnification up to 25.00k×, was used to investigate and view small structures on the surface of the HNT and TPU-HNTs nanocomposites samples. The FESEM was equipped with high resolution images and had insignificant charging effects on the sample surface at a very high spatial resolution of about 1.50 nm, which was 3–6 times that of the TEM. The thermal properties of the samples were investigated using a Thermogravimetric analyser; model Q600, a product of TA Instruments, New Castle, US with heating rate of 10 °C per minute. The mixture of the nanocomposites was performed with a Brabender mixer (Model W 50 EHT) Corder PL 2000 compounder equipped with a 50 cm^3 kneader chamber. For the preparation of specimens for testing, the injection apparatus DSM Xplore moulding injection machine was used. The heating chamber of 10 cm^3 can be heated up to 350 °C. To investigate tensile strength and strain, an Instron Universal Testing Machine (INSTRON 5567) was used.

3.3. Preparation of the Sample

The drying process of the TPU and HNTs was carried out in an oven at a temperature of 80 °C for 12 h.[36] Following drying, the TPU-HNTs nanocomposites were homogenized using a Brabender mixer.[27, 37] The matrix was mixed until stabilization of the torque and was followed by adding filler into the mixer. The mixture was then injected using a moulding machine, whereby four samples were produced including the neat sample, as shown in Figures 11(a)–(d) at loading percentages of 0 (neat TPU), 1, 2 and 3 wt.% HNTs, respectively. The fourth sample was prepared using the optimized parameters for tensile strength and tensile strain at 190 °C, 30 rpm, 30 min, and 1 wt.% HNTs loading. The dimensions of the samples are shown in Figure 11(e).

Table X. Physical properties of HNTs.

Chemical formula	Surface area (m^2/g)	Pore volume (mL/g)	Density (Kg/m^3)	Refractive index
$Al_2Si_2O_5(OH)_4 \cdot nH_2O$	65	~1.25	2540	1.54

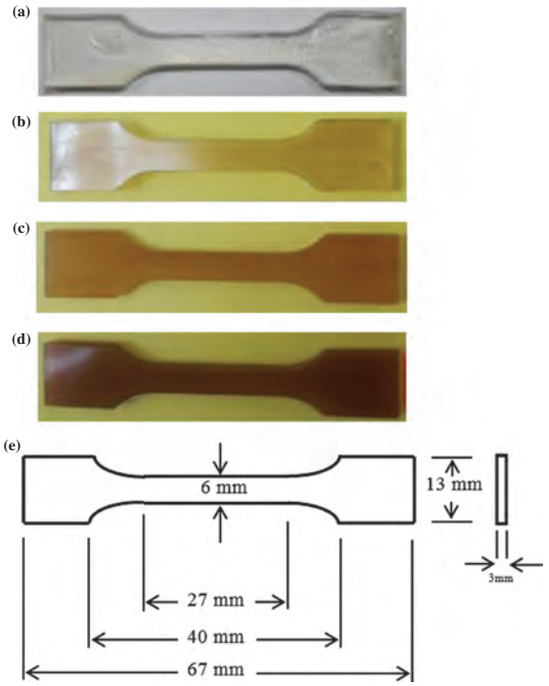

Fig. 11. Samples of TPU-HNTs nanocomposites (a) neat TPU, (b) 1 wt.%, (c) 2 wt.% and (d) 3 wt.%, and (e) sample dimensions.

4. CONCLUSIONS

The technology of the nanocomposites is a relatively new technology which still faces many technical challenges that extend from a merely preparation of the samples to comprehensive theoretical approach. The switching from carbon nanotubes to HNTs–the cheaper- has influenced industry by producing better nanocomposites with special physicochemical and mechanical properties. In this work, Taguchi's design of experiment was implemented to minimize the number of experiments by optimizing the controlled parameters and their relevant levels. Additionally, ANOVA statistical approach was also used for better correlation among the optimized trials. The tested samples in this work include the neat TPU, as standard, TPU-1 wt.% HNTs, TPU-2 wt.% HNTs, TPU-3 wt.% HNTs, and a sample that shows the optimization of tensile strength and tensile strain. The parameters of 190 °C, 30 rpm, 20 min and 1 wt.% HNTs loading are the most important parameters for optimizing the mechanical properties of TPU enforced by HNTs. ANOVA analysis has shown that the 1 wt.% HNTs loading is the most important factor for optimizing the mechanical properties while other parameters have less influence. These results were tested using

FESEM and TGA where the investigation has shown again a very good agreement with Taguchi and ANOVA. The measurements of the tensile strength and tensile strain have shown improvement of 42% and 144% due to a loading of 1 wt.% HNTs, respectively. On contrary to these important results, TGA has shown little effect on the degradation of the nanocomposite sample which suggests that the TPU crystal does not undergo deformation due to the treatment.

APPENDIX A

Step 1: *Selection of factors using Taguchi design*:

Four factors were chosen at three levels each, as shown in Table A1, and nine experiments were chosen using Taguchi design.

Step 2: *The combination of parameters on the orthogonal* L_9 (3^4) *array*:

Each of the nine experiments was run at four factors as proposed by the Tagchi design. The data in Table II show the optimizing factors of tensile strength, Young's modulus, and tensile strain, classified and arranged by Mintab.

Step 3: *Calculation of the average of each response (tensile strength, Young's modulus, and tensile strain)*:

In order to calculate the average tensile strength, Young's modulus and tensile strain, nine experiments were run at optimizing parameters, which resulted in nine samples. Each sample was divided into three specimens and each specimen was tested for each of the three responses and finally the average value was calculated, as shown in Table A2 for tensile strength; Table A3 for Young's modulus; and Table A4 for tensile strain.

Step 4: *Calculation of* S/N:

This step was to determine the S/N ratio for each response of the tensile strength, Young's modulus, and tensile strain. First, the mean-square deviation (MSD) was calculated according to Eq. (A1):

$$\mathrm{MSD} = \frac{\sum_{i=1}^{n} 1/y_i^2}{n} \tag{A1}$$

where y_i the value of tensile strength for the ith test is; n is the number of tests. An example of calculating MSD is shown as follows:

$$\mathrm{MSD} = \frac{(1/25.493^2) + (1/24.886^2) + (1/25.381^2)}{3} = 0.002$$

Finally, the S/N ratios were calculated according to Eq. (A2):

$$S/N_{LB} = -10\log(\mathrm{MSD}) \tag{A2}$$

As an example of an S/N ratio:

$$S/N_{\mathrm{LB}} = -10\log(\mathrm{MSD}) = 28.0464$$

The average of the responses of the tensile strength, Young's modulus, and the tensile strain and their relevant S/N ratios are collectively shown in Table III.

Step 5: *The procedure in steps 1 through 4 was repeated for all factors and the results are shown in Table V.*

Table A1. The parameters for three levels of selected factors.

Factors	Level 1	Level 2	Level 3
Mixing temp. (°C)	190	200	210
Mixing speed (rpm)	30	40	50
Mixing time (min)	20	30	40
HNTs loading (wt.%)	1	2	3

Table A2. Calculation of the average of tensile strength.

No. run	Mixing temp.	Mixing speed	Mixing time	HNTs loading	Rep 1	Rep 2	Rep 3	Average
1	190	30	20	1	25.49	24.88	25.38	25.25
2	190	40	30	2	16.78	22.93	17.80	19.17
3	190	50	40	3	16.89	15.66	14.82	15.79
4	200	30	30	3	16.85	16.37	17.16	16.79
5	200	40	40	1	19.63	18.90	18.63	19.05
6	200	50	20	2	17.54	17.39	17.70	17.54
7	210	30	40	2	21.36	20.57	21.80	21.24
8	210	40	20	3	13.85	12.18	13.36	13.13
9	210	50	30	1	20.74	20.34	22.33	21.13

Table A3. Calculation of the average of young's modulus.

No. run	Mixing temp.	Mixing speed	Mixing time	HNTs loading	Rep 1	Rep 2	Rep 3	Average
1	190	30	20	1	2.40	5.00	2.96	3.45
2	190	40	30	2	8.46	3.92	7.23	6.54
3	190	50	40	3	10.71	11.33	9.55	10.53
4	200	30	30	3	9.68	10.41	10.26	10.12
5	200	40	40	1	8.58	7.28	7.46	7.77
6	200	50	20	2	7.60	8.17	8.39	8.05
7	210	30	40	2	5.36	6.87	5.92	6.05
8	210	40	20	3	11.30	11.42	11.90	11.54
9	210	50	30	1	6.62	5.89	4.38	5.63

Table A4. Calculation of the average of tensile strain.

No. run	Mixing temp.	Mixing speed	Mixing time	HNTs loading	Rep 1	Rep 2	Rep 3	Average
1	190	30	20	1	997.1	1054.0	1101.0	1050.7
2	190	40	30	2	989.5	971.9	1010.0	990.4
3	190	50	40	3	590.5	615.7	618.4	608.2
4	200	30	30	3	682.4	672.3	687.6	680.7
5	200	40	40	1	1029.5	1008.0	1009.0	1015.5
6	200	50	20	2	890.4	843.3	876.7	870.1
7	210	30	40	2	1004.2	994.6	1019.0	1005.9
8	210	40	20	3	506.8	499.4	519.7	508.6
9	210	50	30	1	1056.4	1046.0	989.1	1030.5

Conflicts of Interest

The authors declare no conflict of interest.

Acknowledgments: The authors thank Universiti Kebangsaan Malaysia and the Ministry of Higher Education for the financial support grant DIP-2014-006 and LRGS/TD/2012/USM-UKM/PT/05.

References and Notes

1. Y. Dong, T. Bickford, H. J. Haroosh, K.-T. Lau, and H. Takagi, *Applied Physics A* 112, 747 **(2013)**.
2. M. Liu, B. Guo, M. Du, F. Chen, and D. Jia, *Polymer* 50, 3022 **(2009)**.
3. J. S. Pang, M. Ansari, O. S. Zaroog, M. H. Ali, and S. Sapuan, *HBRC Journal* 10, 138 **(2014)**.
4. E. Joussein, S. Petit, J. Churchman, B. Theng, D. Righi, and B. Delvaux, *Clay Minerals* 40, 383 **(2005)**.
5. C. C. Harvey and H. H. Murray, *Clay Miner. Soc. Spec. Pub.* 233 **(1990)**.
6. Z. Jia, Y. Luo, S. Yang, B. Guo, M. Du, and D. Jia, *Chinese Journal of Polymer Science* 27, 857 **(2009)**.
7. K. P. Rajan, N. Veena, P. Singh, and G. Nando, *Yanbu J. Eng. Sci.* 1, 59 **(2010)**.
8. B. Finnigan, D. Martin, P. Halley, R. Truss, and K. Campbell, *Polymer* 45, 2249 **(2004)**.
9. A. Pattanayak and S. C. Jana, *Polymer* 46, 3275 **(2005)**.
10. Y. A. El-Shekeil, S. Sapuan, M. Azaman, and M. Jawaid, *Advances in Materials Science and Engineering* 2013 **(2013)**.
11. C. Lai, S. Sapuan, M. Ahmad, N. Yahya, and K. Dahlan, *Polymer-Plastic Technology and Engineering* 44, 619 **(2005)**.
12. M. Gholami and G. Mir Mohamad Sadeghi, *Journal of Particle Science and Technology* 1, 1 **(2015)**.
13. S. Shokoohi, A. Arefazar, and G. Naderi, *Materials and Design* 32, 1697 **(2011)**.
14. R. K. Roy, Design of experiments using the taguchi approach, 16 Steps to Product and Process Improvement, John Wiley & Sons **(2001)**.
15. K. Prashantha, J. Soulestin, M. Lacrampe, E. Lafranche, P. Krawczak, G. Dupin et al., *Express Polym. Lett.* 3, 630 **(2009)**.
16. M. Rafizadeh, J. Morshedian, E. Ghasemi, and A. Bolouri, *Iranian Polymer Journal* 14, 881 **(2005)**.
17. R. Yang, R. Mather, and A. Fotheringham, *Journal of Materials Science* 36, 3097 **(2001)**.
18. S. K. Park, K. Do Kim, and H. T. Kim, *Colloids and Surfaces A: Physicochemical and Engineering Aspects* 197, 7 **(2002)**.
19. J. Liu, P. Lu, and W. Weng, *Materials Science and Engineering: B* 85, 209 **(2001)**.
20. N. M. Mehat and S. Kamaruddin, *Journal of Materials Processing Technology* 211, 1989 **(2011)**.
21. M. Azaman, S. Sapuan, S. Sulaiman, E. Zainudin, and A. Khalina, *Polymer Engineering and Science* 55, 1082 **(2015)**.
22. X. Wang, G. Zhao, and G. Wang, *Materials and Design* 47, 779 **(2013)**.
23. E. Hakimian and A. B. Sulong, *Materials and Design* 42, 62 **(2012)**.
24. R. Klimkiewicz and E. B. Drąg, *Journal of Physics and Chemistry of Solids* 65, 459 **(2004)**.
25. E. Joussein, S. Petit, and B. Delvaux, *Applied Clay Science* 35, 17 **(2007)**.
26. L. Pizzatto, A. Lizot, R. Fiorio, C. L. Amorim, G. Machado, M. Giovanela, et al., *Materials Science and Engineering: C* 29, 474 **(2009)**.
27. A. Toldy, G. Harakály, B. Szolnoki, E. Zimonyi, and G. Marosi, *Polym. Degrad. Stab.* 97, 2524 **(2012)**.
28. P. Russo, D. Acierno, G. Marletta, and G. L. Destri, *Eur. Polym. J.* 49, 3155 **(2013)**.
29. L. Bartolomé, J. Aurrekoetxea, M. A. Urchegui, and W. Tato, *Materials and Design* 49, 974 **(2013)**.
30. Y. El-Shekeil, S. Sapuan, A. Khalina, E. Zainudin, and O. Al-Shuja'a, *Express Polymer Letters* 6 **(2012)**.
31. A. B. Sulong, T. S. Gaaz, and J. Sahari, *Procedia-Social and Behavioral Sciences* 195, 2748 **(2015)**.
32. A. K. Barick and D. K. Tripathy, *Composites Part A: Applied Science and Manufacturing* 41, 1471 **(2010)**.
33. M. Ulcnik-Krump and L. De Lucca Freitas, *Polym. Eng. Sci.* 44, 838 **(2004)**.
34. J. Marini, E. Pollet, L. Averous, and R. E. S. Bretas, *Polymer* 55, 5226 **(2014)**.
35. P. S. Goh, A. F. Ismail, S. M. Sanip, B. C. Ng, and M. Aziz, *Sep. Purif. Technol.* 81, 243 **(2011)**.
36. J. Bian, H. L. Lin, F. X. He, X. W. Wei, I.-T. Chang, and E. Sancaktar, *Composites Part A: Applied Science and Manufacturing* 47, 72 **(2013)**.
37. M. Sureshkumar, K. Naskar, G. Nando, Y. Bhardwaj, and S. Sabharwal, *Polymer-Plastics Technology and Engineering* 47, 341 **(2008)**.

ARTICLE